

**2025 Structural Evaluation of a Canister Drop inside a Vertical
Concrete Cask**

Mike Yaksh, Ph.D., PE
NAC International INC
Norcross, GA

Suresh Babu, Ph.D.
NAC International INC
Norcross, GA

Abstract

In preparation of lowering a welded canister containing fuel inside a vertical concrete cask (VCC), a bottom end drop of the canister into the VCC is postulated. The VCC is positioned on a trailer designed to move the loaded VCC, and the trailer is supported by a concrete floor. Pertinent to the evaluation are the existence of gaps which could result in secondary impact. Preliminary evaluations confirm that a significant gap could occur between the fuel and the canister bottom plate by the time the canister reached the bottom of the VCC. In addition to the developed gap between the canister and fuel, the trailer which is positioned off the floor could also have a variation in the gap between the floor and the bottom of the trailer. Since the duration of the free fall is at least an order of magnitude larger than the impact duration, two different analytical methods are used in the evaluation of each part of the solution. It is observed that the compliance of the canister has a significant effect on the gap developed between the fuel and the canister in the bottom end drop. Analyses were used to confirm that the canister boundary maintains its integrity in this bottom end drop. It was also observed that in a multibody impact, the ability to absorb energy by intervening components can significantly affect the loads applied to the canister.

Introduction

Regulations defined in 10CFR Part 72 [1] governing the storage of spent nuclear fuel require that the fuel be stored in an inert environment. The confinement boundary of the system described in this paper is a right circular stainless steel canister with a 2.75 inch thick bottom plate and 9 inch thick closure lid. The weld connecting the lid to the canister is defined as the closure weld and is governed by ISG-18 [2]. The canister, without the lid, is initially placed in the spent fuel pool or an adjacent section of the pool and is loaded with 37 PWR assemblies or 87 BWR assemblies. To facilitate welding the closure lid, the canister, which rests in a shielded cask to permit moving the canister, is moved to a work area to allow the closure weld to be made in conjunction with an additional redundant weld. Other operations are performed in this work area to prepare the canister and fuel for storage at a location on site. While the canister is the confinement boundary, the canister is placed into a concrete overpack (concrete cask) for additional shielding as well protecting the canister confinement boundary from accident conditions. The weights and overall dimensions of the canister and concrete overpack

are given in Table 1 below [3].

Table 1. Component Weights and Overall Dimensions

Component	Weight (lb)	Outer diameter (in)	Height (in)
Welded Canister (with fuel assemblies)	94,000	72	185
Concrete overpack (empty)	214,500	136	218

In this design, the loading of the canister (from the shielded transfer cask) into the concrete overpack occurs in the building where the closure operations are performed. The concrete cask rests on a wheeled trailer and is moved into the building. To facilitate loading the canister into the concrete cask, the shielded cask, is first positioned on top of the concrete cask, which rests on the trailer. Upon preparation of the trailer for the loading, the canister is then lowered into the concrete cask. As the canister is being lowered to position it on a pedestal at the base of the cask, the postulated drop occurs, in which the canister impacts the pedestal. The load is then transmitted through the pedestal into the trailer and then to the floor. While the trailer is supported during the loading operation, the posts for the purpose of the evaluation, was excluded from supporting the trailer. This analysis decision resulted in the free fall of the trailer, which would be further accelerated by the force from the impact of the canister onto the pedestal. This acceleration actually separates the concrete cask from the trailer, until the cask then impacts the trailer shortly thereafter. To ensure that bounding conditions were identified, analyses were performed for the gap between the floor and the bottom of the trailer to vary between three and four inches. Two sets of analyses were performed; a trailer-floor gap of 3 inches and a trailer-floor gap of 4 inches.

Concrete cask/canister/trailer Finite Element Model

The structural evaluation uses the explicit dynamics code, LS-DYNA [4] to determine the response of the components of the system. As such, the finite element model was generated that was appropriate for the explicit finite element methodology. The complete finite model for this evaluation consisted of the following components.

- 1) Vertical concrete cask
- 2) Canister
- 3) Fuel/basket contents inside the canister
- 4) Trailer to move the concrete cask to the storage pad
- 5) Concrete floor

The complete finite element model is shown in Figure 1. The concrete cask, canister and trailer have quarter symmetry designs, which would permit a quarter symmetry model. In reviewing the floor to be impacted by the trailer, the model of the floor had only a single plane of symmetry. Therefore the model shown in Figure 1 is a half symmetry model of all the components.

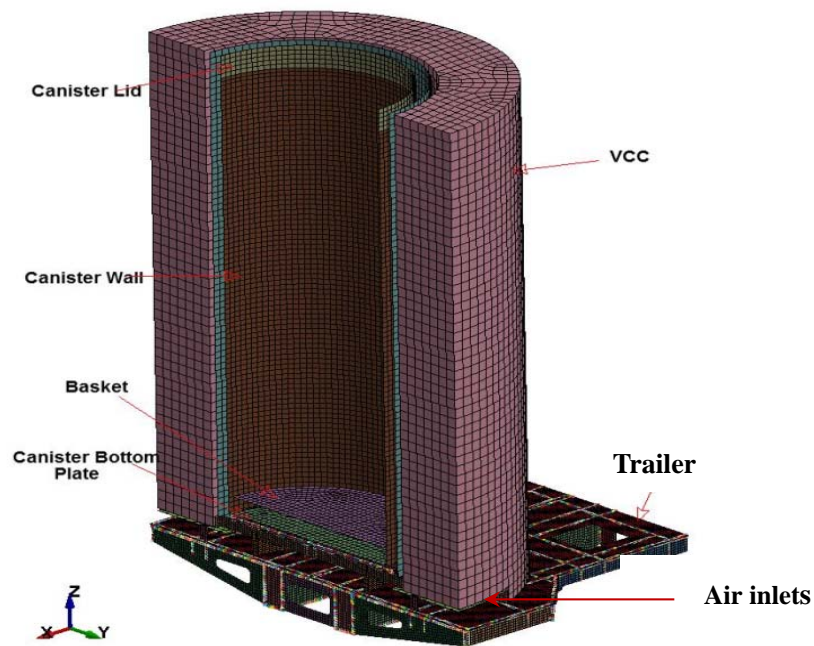


Figure 1. Finite Element Model

The purpose of the model in this paper is to evaluate the structural behavior of the canister. The 2.75 inch thick canister bottom plate and the ½ inch thick 72 inch canister outer diameter shell were comprised of shell elements in the model. One advantage of the shell elements is that increasing the accuracy of the stress through the thickness could easily be accomplished by increasing the number of integration points through the shell thickness as opposed to regeneration of the parts with increased number of elements through the thickness. The canister lid is 9 inches thick and is welded to the canister shell with the two groove welds. The thicker 0.5 inch weld is the closure weld, while the adjacent weld provides redundant closure in terms of a leakage path from the canister cavity. Due to the position of the weld between the lid and shell, the weld is subjected to shear. As will be described in the criteria section, the shear stresses in the weld in this accident condition has a separate criteria from the shells which are subjected to both membrane and bending stresses. The lid has a weight of approximately 10,000 pounds, which will generate a significant inertial load to be transmitted to the shell. The mass of the lid is modeled with the shell elements at the elevation of the lid using a density to represent the total mass of the lid. This method was selected, since the weld shear stress could be accurately determined using the acceleration at the location of the lid. The use of significantly smaller elements for the weld to characterize the shear was not required. To validate this methodology, an additional sensitivity study was performed. The contents of the canister were modeled as a half circular plate of shell elements with the mass of the basket and fuel. The evaluation of the canister did not require a detailed model of the fuel and basket.

As a result of the canister drop, the canister will impact the pedestal. The pedestal is comprised of a thick circular plate having the diameter of the canister which is supported by a series of carbon steel

beams. These beams are attached to the 2.5 inch thick inlet plates that form the top surface of the inlet shown in Figure 1. These components are modeled using shell elements. The beams are modeled with sufficient elements to simulate their buckling during the impact. As a result of the pedestal deformation, the pedestal acts as a component which absorbs energy.

The concrete cask is comprised of 26 inch thick shell of concrete with a thick carbon steel shell at the inner radius of the cask. Their dimensions are controlled by shielding requirements. The concrete is not expected to affect the performance of the canister, but provides significant load to the trailer in the secondary impact of the trailer with the floor. The air inlets shown in Figure 1 have a thick top plate for shielding and are supported by shielding plugs. These cylindrical bars are for shielding, but in the impact of the concrete cask, they support the inner radius of the inlet that maintains the position of the beams of the pedestal.

The trailer is also shown in Figure 1. Since it is fabricated from plates, it was modeled with shell elements. During operation, the trailer is supported by posts attached to the trailer. These posts rest on the concrete floor. The posts, due to their stiffness and ductility, would mitigate the secondary impact of the trailer with the floor, in addition to absorbing energy. To avoid qualification of the posts, it was conservative to treat the posts as having no strength to resist the motion of the trailer upon impact of the canister. The trailer was modeled with an initial gap between the bottom of the trailer and the top of the floor. The floor was also modeled in detail to represent its stiffness and contribution to the loads applied to the trailer, but is considered to be outside the scope of this paper. The model of the concrete cask, canister and trailers consisted of approximately 68,000 elements, and the element counts associated with each component are shown in Table 2 below.

Table 2. Number of Element for Model Components

Component	Number of Elements
Trailer	32,908
Concrete / cask liner	20,912
Concrete cask pedestal/inlet	7,906
Canister Assembly	6,538
Total Number of Elements	68,264

The model for the trailer was imported from a CAD model and the shell elements were positioned at the midplane of each component. The concrete cask and canister model were generated in ANSYS [5] and imported into LS-DYNA and combined into a single model along with the model of the floor and the trailer. All material properties utilized stress-strain curves to permit the inelastic behavior of the components to be simulated. The contact options with in LS-DYNA were used to simulate the nonlinear behavior of the components as well as the self-contact of the shell elements forming the pedestal as it underwent buckling.

Structural Criteria

As a result of the impact of the canister with the concrete cask pedestal there will also be an ensuing impact with the trailer and the floor, all components will be loaded. The criterion of interest in this paper is associated with the canister. The canister is evaluated against Section III Division 1, Appendix F [6]. As per Subsection F-1341.2, where the component is evaluated on a plastic basis the following primary stress limits shall be applied.

- (a) The general primary membrane stress intensity P_m shall not exceed greater of $0.7S_u$ and $S_y + 1/3(S_u - S_y)$ (49.7 ksi corresponding to the temperature at the bottom of the canister).
- (b) The maximum primary stress intensity (SI_{max}) at any location shall not exceed $0.9S_u$ (63.9 ksi corresponding to the temperature at the bottom of the canister).
- (c) The average primary shear across a section loaded in pure shear shall not exceed $0.42S_u$. (26.9 ksi corresponding to the temperature at the top of the canister).

Items a) and b) are applied to the shell and bottom canister plate. The closure weld connects the 9 inch thick lid to the shell and is subjected to shear which is evaluated using Item c). As a comparison, the results are also used to determine the safety factors using strain based criteria in Section III Division 3, WC-3700 [7]. The concrete cask pedestal and trailer will experience significant plastic strain, but it is not intended to remain intact. A structural criterion is not applied to either of these structures. The evaluation of the floor integrity was considered separately and is not presented in this paper.

Determination of the Fuel/Basket-Canister Gap

At the time of the postulated canister drop, the fuel and basket are resting on the bottom canister plate while the top of the canister is attached to a hook. While the fuel weight is distributed over the bottom plate, the basket is being primarily supported at the basket periphery. The load applied to the canister bottom plate results in strain energy being developed in the shell wall and canister bottom plate. The sudden release of the canister from the crane hook allows the shell and bottom plate to respond. Depending on the relative stiffness's of the fuel/basket and canister shell, a differential velocity between the two can develop. As a result, a gap between the fuel/basket and bottom plate will develop and increase as the canister drops through a height of 18 feet. The significance of this gap is that the canister bottom plate will impact the concrete cask pedestal followed by the impact of the fuel basket onto the canister bottom plate which will already have undergone plastic deformation due to the canister impact. To determine the sensitivity of this gap to the shell and fuel stiffness, a series of transients were solved using the 2D axisymmetric model in Figure 2. The attachment points to the lid were represented by displacement constraints on the top of the shell. An initial load step was solved with gravity as a static condition. The drop condition was then initiated by the sudden removal of the vertical constraints. The solution of this free fall was performed using the implicit methodology in ANSYS [5]. The shell thickness was varied as well as the axial stiffness of the fuel.

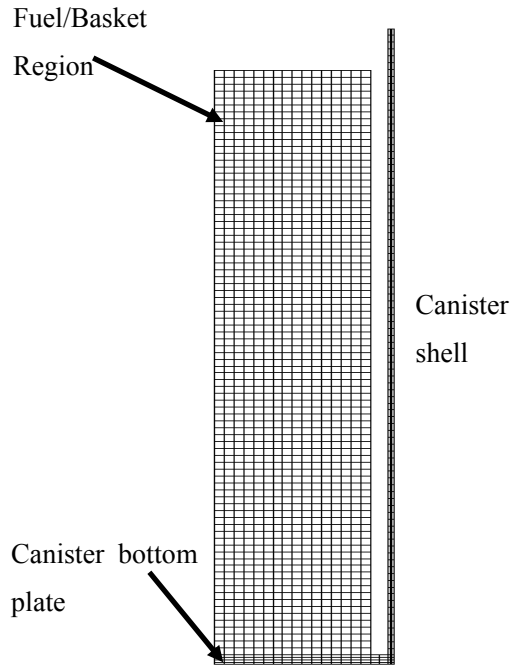


Figure 2. Simple Model to Determine the Fuel/Basket-Canister Plate Gap

Instead of reporting the gap at the time of impact in terms of the shell thickness, the fundamental axial modal frequency was computed associated with the shell thickness. The properties of the fuel elements were varied to have a fundamental mode of 150 Hz, 230 Hz and 400 Hz. The fuel rod fundamental frequency, depending on the degree in which the pellet is attached to the cladding, could range from 160 Hz to 400 Hz. The basket/canister gaps versus shell frequencies are shown in Table 3 below for an 18 foot drop.

Table 3. Effect of Contents/Shell Frequencies on Basket/Fuel-Canister Plate Gap

Shell Frequency (Hz)	Canister/Basket – Bottom Canister Plate Gap (in)		
	Frequency (Hz) 160	Frequency (Hz) 230	Frequency (Hz) 400
73	0.03	4.7	4.6
89	0.02	3.8	3.7
103	0.011	3.1	3.1
115	0.01	<0 .01	2.7
126	<0.01	< 0.01	<0.01

The results show the gap at the time of impact is sensitive to both the shell and fuel frequencies. If each fuel assembly is assumed to be independent, there is basically no gap. If the fuel rods are assumed to remain fixed to the fuel grids, the fundamental mode based on the water tubes supporting the fuel would result in even a lower frequency than 160 Hz also indicating that the gap is insignificant.

Since the fuel frequency is not easily confirmed, the analyses were performed with the maximum gap. For the actual canister in the model, the maximum gap is computed to be 4.3 inches.

Boundary Conditions for the Solutions with the Complete Model

Since this is a half symmetry model, the plane of symmetry was appropriately constrained. The concrete cask was positioned on the trailer in contact with the trailer. The canister was positioned above the pedestal plate with a small gap. For an 18 feet drop, the initial velocity of the canister and the contents was 408.5 in/sec. The basket fuel model was positioned 4.3 inches above the bottom canister plate with the same initial velocity. The trailer and concrete cask had no velocity specification. The gravity body force load was suddenly applied to the entire model. This provided a conservative loading of all the self-weights of the concrete floor and components. More importantly, this was essential to obtain the correct acceleration of the components to determine the secondary impact velocities of the basket/fuel against the canister bottom plate and the trailer against the floor.

Results for the Drop Analyses for the 4.3 inch Basket/Fuel-Canister Gap

The impact of the canister and contents is actually a series of impacts involving the canister and contents, the concrete cask pedestal, the concrete cask, the trailer and the floor. This series of events are reflected in Figure 3 which is the force time history applied to the floor by the trailer and can be summarized in the follow events:

- 1) Canister bottom plate impacts the concrete cask pedestal plate, which begins to load the trailer through the pedestal. At the instant the analysis is initiated, the trailer begins to free fall, but received additional force to accelerate the trailer towards the floor. This causes the trailer to separate from the concrete cask outside the pedestal area.
- 2) The trailer impacts the floor at 17 ms.

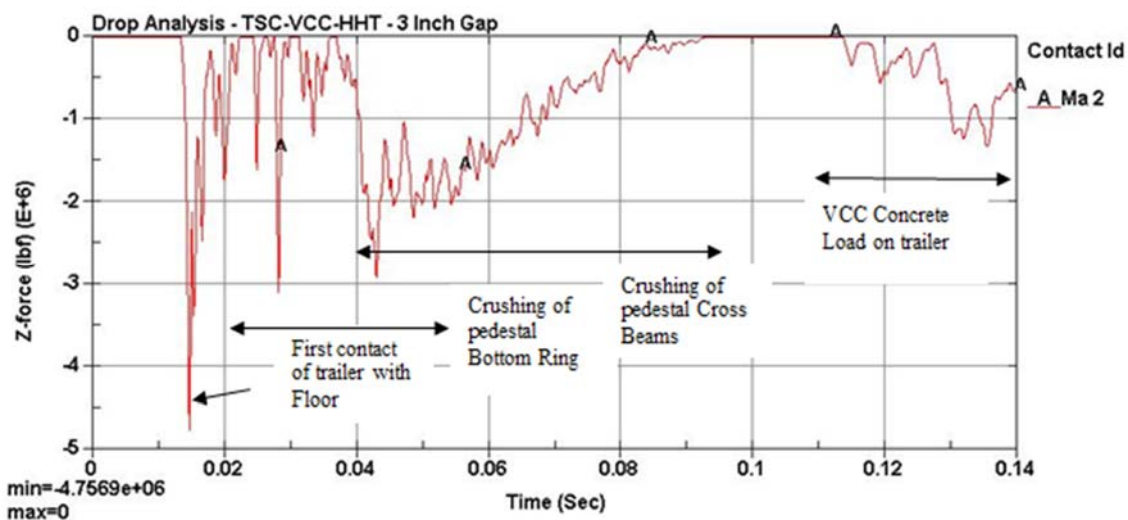


Figure 3. Time History of Force Applied to the Floor

- 3) The canister contents impacts the bottom plate after the trailer impacts the floor. This causes additional deformation to the pedestal.
- 4) Pedestal collapse is initiated at 40 ms Pedestal collapses at 80 ms
- 5) Concrete cask impacts the trailer at 100 ms

Note that some of the spikes have a duration less than 1 ms. Once the pedestal begins to collapse, the force to the floor decreases during the 40 ms duration. The deformation of the pedestal acted as an energy absorber to limit the deceleration of the canister. This behavior was observed for all the solutions of the model using different trailer-floor gaps.

The largest canister plastic strain occurs for the 3 inch trailer-floor gap. The plot of the plastic strain for the 3 inch trailer-floor gap is shown in Figure 4.

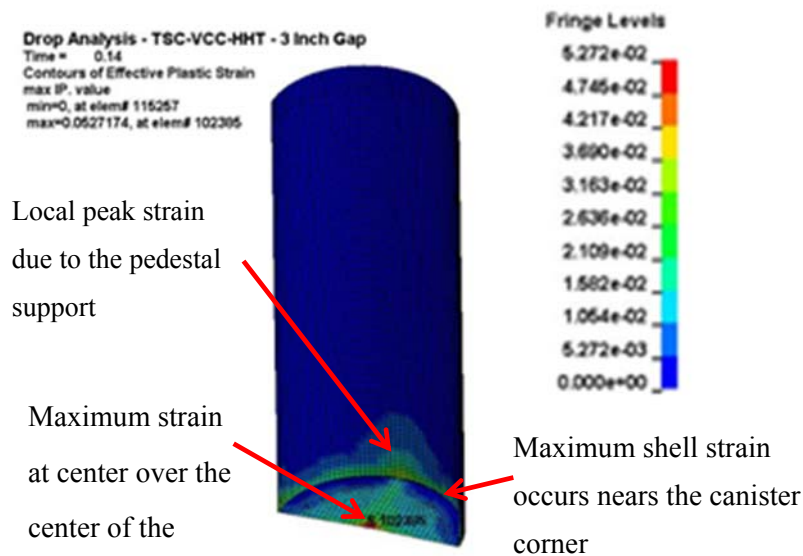


Figure 4. Plastic Strain for the 3 inch Trailer-Floor Gap

The peak strain occurs at the center of the bottom plate which is remote to the discontinuity of the corner. The peak strain in the shell occurs near the discontinuity. The strain associated with the loading of the canister lid is minimal. In using Section III Division 1, Appendix F the peak surface stress intensity (Engineering), and average through the thickness are needed. Since the data is being extracted from shell elements, the peak stresses are extracted from the outer integration point and extrapolated to the surface. The output from the solution is in terms of true stress and true strain. These quantities are converted to engineering quantities to allow comparison with the stress allowables in Division 1.

The results represented as factors of safety for the 3 inch trailer gap are shown in the Table 4 below. The closure weld requires an additional reduction factor of 0.8 against the stress allowable [3]. The above safety factor applied the entire load to the single closure weld and did not include any load transmitted by the adjacent weld, just above the closure weld, which is a redundant weld. Using both welds would have resulted a SF closer to 2.

Table 4. Safety Factors (SF) for the Canister for the Base Model for the 3 inch and 4 inch trailer-floor gap using the Stress Based Criteria in Section III Division 1

Appendix F

Case	SF for Bottom canister plate $S_{I_{max}}$	SF for Bottom canister plate P_m	SF for Shell $S_{I_{max}}$	SF for Shell P_m	SF for Closure weld Shear
3 inch trailer-floor gap	1.13	2.15	1.16	1.10	1.14

Section III Division 3 WC-3700 provides strain criteria [7]. While this method is not commonly accepted in the regulatory environment, it does provide a more accurate assessment in terms of the true capacity of the canister. The 18 foot drop of the canister is a energy limited event which is the type of loading the criteria in WC-3700 is to address, which has been described in numerous papers [8], [9].

The strain at the center of the canister plate is considered to be away from a discontinuity peak strain and the criteria for the equivalent strain (ϵ) is defined in terms of an average plastic strain and a peak strain as:

- 1) Average strain through a section

$$TF \times (\epsilon_{ave}) \leq 0.67 \epsilon_{uniform}$$

- 2) Maximum strain of the section

$$TF \times (\epsilon_{max}) \leq \epsilon_{uniform} + 0.25(\epsilon_{fracture} - \epsilon_{uniform})$$

The strain at the shell corner of the canister plate is considered to be at a discontinuity and the criteria for the equivalent strain (ϵ) is defined in terms of an average plastic strain and a peak strain as:

- 1) Average strain through a section

$$TF \times (\epsilon_{ave}) \leq 0.85 \epsilon_{uniform}$$

- 2) Maximum strain of the section

$$TF \times (\epsilon_{max}) \leq \epsilon_{uniform} + 0.25(\epsilon_{fracture} - \epsilon_{uniform})$$

The quantity TF is defined as a Triaxiality Factor to account for the influence of multiaxial state of stress on failure. The TF defined in section WC-3700 is

$$TF = \frac{\sigma_1 + \sigma_2 + \sigma_3}{\sqrt{\frac{1}{2}[(\sigma_1 - \sigma_2)^2 + (\sigma_2 - \sigma_3)^2 + (\sigma_1 - \sigma_3)^2]}}$$

ASME Section VIII Division 2 Part 5 [10] also defines a TF which factors the maximum allowable strain, but it is significantly different than the above definition. Additionally the TF definitions used in the computer code being used needs to be reviewed to determine whether the first stress invariant (S_1) is being used (as shown above) or the pressure ($S_1/3$) is being used to compute the TF by the post processor.

For the bottom plate material, the material strains needed for the criteria is, $\epsilon_{\text{uniform}} = 40\%$ and $\epsilon_{\text{fracture}} = 52\%$. These were extracted for the temperature at the bottom of the canister.

The TF must be extracted as a time history of the element for the strain of interest. It is noted that the TF is dependent on the stress state. This implies that the TF could be different for each strain quantity (average versus peak). Moreover, the TF can vary significantly with respect to time as shown in Figure 5. Figure 5 is the ratio of the S_1 to the equivalent stress.

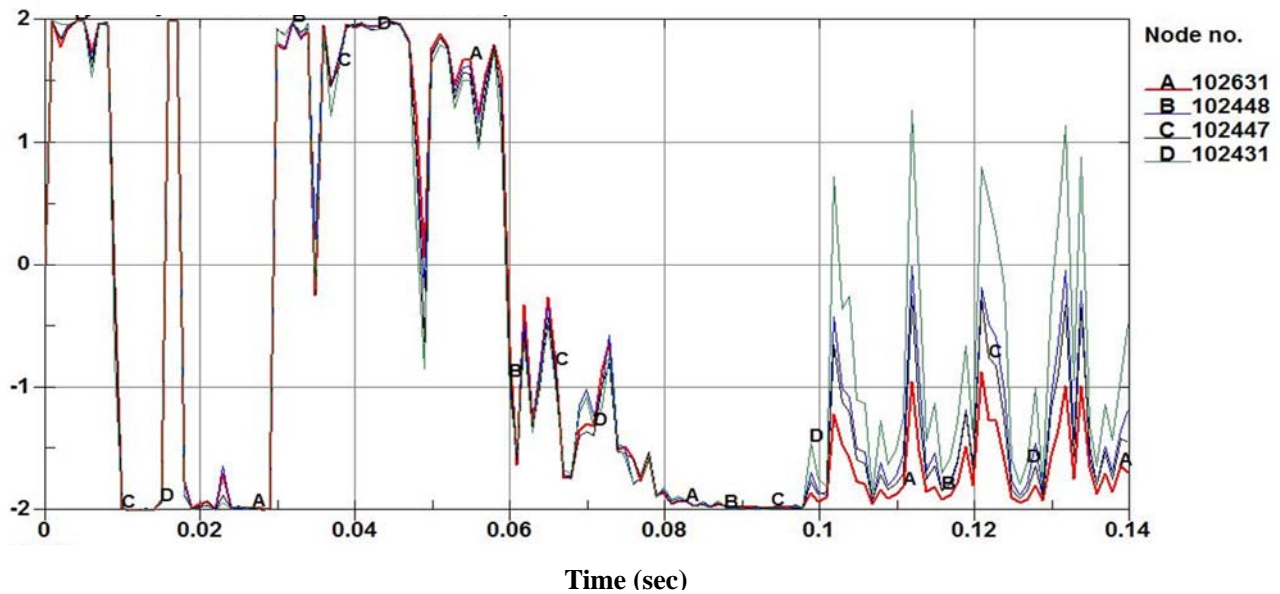


Figure 5. Section III Division 3 Triaxiality Factor for Upper Surface of Canister Plate

This indicates that the Safety Factor (SF) can vary in a similar manner as the time history plot for TF, since plastic strains are not subject to such drastic variations. Since S_1 is a signed quantity, it can be negative, but values of TF less than +1 are restricted to being unity. This is a significant difference from stress based criteria in which the allowable stresses do not vary with time in a constant temperature environment. In using the strain based criteria, fabrication strain need only be considered, if they exceed 5%. Using the expression in [7], the strain of shell is 0.7% confirming that it need not be furthered considered. The Safety Factors (SF) are the ratios of the maximum allowable strain to the factored strains (e.g., $TF \times (\epsilon_{\text{max}})$) and are shown in Table 5 below along with the associated TF. In comparing the results of the two criteria, the strain base criteria shows a significant SF as compared to the stress based criteria. Moreover the location changes between the two criteria. The TF values near 2 indicate that the state of stress at each location is essentially a biaxial stress state (Table EE-1150-1 in (Section III Appendices in [7])). This is consistent with the bending of the bottom canister plate about two horizontal axes and the shell having both a hoop stress and an axial stress. The strain based criteria offers many advantages, but the effort to obtain the $TF \times \epsilon$ could be significant.

Table 5 Safety Factors (SF) for the Canister for the Base Model for the 3 inch trailer-floor gap using the Strain Based Criteria in Section III Division 3

Case	Bottom canister plate TF×(ε _{max})		Bottom canister plate TF×(ε _{ave})		Shell TF×(ε _{max})		Shell TF×(ε _{ave})	
	SF	TF	SF	TF	SF	TF	SF	TF
	3 inch trailer-floor gap	4.45	1.94	3.95	1.93	4.90	1.96	4.66

For each of the solutions generated, certain energies were reviewed. Figure 8 shows the energies of interest and Table 6 below summarizes the results and observations of the energies.

Table 6 Energies Post Processed for the Solutions

Energy	Curve in Figure 6	Observation
Kinetic	A	Verify initial KE is correct and minimal KE is in the solution
Hourglass	D	Confirms that the hourglass energy to less than 5%
Sliding energy	E	Confirms that the contacts in the model are simulating the contact correctly without nodes being “stuck” to the target or target penetration
External Work	F	Product of node displacement and force to confirm that the material model and element > 0 (else inconsistent element behavior is occurring)

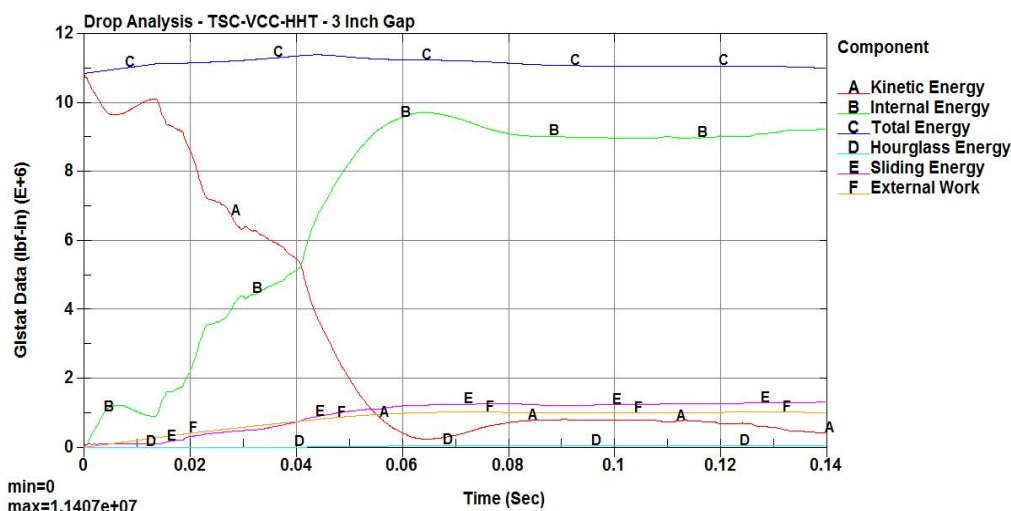


Figure 6. Energy Plots for the 3 inch Trailer-Floor Gap

Drop results for Additional Sensitivity Studies

It was of interest to observe the effect of the basket/fuel-canister bottom plate gap on the strains developed in the canister due to the impacts. The above model was used to allow the basket/fuel-canister bottom plate to take on values of 2.25 and 0.01 inches for the initial position of the fuel/basket

inside the canister. The maximum strains in the canister bottom plate and in the shell occurred in the same location as for the base case. The SF for the closure weld was computed as before. These results are summarized in Table 7 below.

Table 7. Strain Results for the Additional Cases of Contents/Canister Gaps

Basket/fuel-canister gap	Canister plate Peak Strain (%)	Bottom canister Peak Strain (%)	SF for Closure weld
4.3 (base case)	5.27	4.47	1.14
2.25	4.11	3.46	1.30
0.01	1.81	1.37	3.20

The results are as expected in that the strains would decrease and the SF for the closure weld would increase. Since the state of stress is not expected to change due to the size of the gap, this implies that the SF based on the strains would increase to values over 10. This indicates that the secondary impact needs to be considered. Depending on the stiffness’s of the shell and the contents, it could be significant. Another sensitivity study was performed to evaluate the effect of the lid response. In this solution, the model having the 3 inch trailer-floor gap in conjunction with the maximum basket/fuel-canister gap (4.3 inches) was used. The base model was altered to include a 9 inch thick lid. It is connected to the shell at the location of the closure weld using a constraint of the closure nodes of the weld to the adjacent elements on the canister shell. The output from the solution was the vertical force in the constraint which was used to compute a shear force acting on the weld. The closure weld is considered to be in shear and for Appendix F it is limited to 0.42Su. Comparison of the two results are shown in Table 8 below

Table 8. Comparison of Results for the Base Case with the Modeled Lid

Basket/fuel-canister gap	Canister plate Peak Strain (%)	Canister Shell Peak Strain (%)	SF for Closure Weld
Lid not explicitly modeled	5.27	4.47	1.14
Lid modeled	5.08	4.55	1.69

In the base model, the lid mass is modeled in the canister shell (at the top) which would result in the lid mass participating 100% for each time step of the solution. In modeling the lid explicitly, this dynamic behavior of the lid does not occur. The results suggest that considering the lid mass to participate 100% for each time step is conservative for the peak canister strain as well as for the closure weld. The slight increase of the canister shell strain is not considered to be the controlling location based on the larger strain in the bottom canister plate.

Conclusion

This paper describes the simulation of a multibody impact of the canister contents, the canister, the concrete cask and the trailer with a floor as the loaded canister is dropped into a concrete cask. The effects of the gap sizes for the canister contents and the trailer-floor gap were assessed. The canister contents gap at the time of impact is found to be dependent on the stiffness's of both the contents and the canister. The trailer floor gap affects the trailer deformation and energy absorption which in turns affects the canister response. The use of Section III Division 3 strain criteria indicates that the confinement boundary has significant factors of safety for stainless steel canister materials as compared to the Section III Division 1 (Appendix F) stress criteria. The evaluations confirmed that the canister confinement boundary remains intact for the 18 foot drop of the loaded canister into the concrete cask.

References

- [1] 10 CFR Part 72, "Licensing Requirements for the Independent Storage of Spent Nuclear Fuel, High Level Radioactive Waste, and Reactor-Related Greater than Class C Waste", United States Nuclear Regulatory Commission, Washington, D.C.
- [2] Division of Spent Fuel Storage and Transportation, Interim Staff Guidance – ISG-18 Rev 1, "The Design and Testing of Lid Welds on Austenitic Stainless Steel Canisters as the Confinement Boundary for Spent Fuel Storage", United States Nuclear Regulatory Commission, Washington, D.C.
- [3] MAGNASTOR Final Safety Analysis Report, July 2015, Revision 7, Docket No. 72-1031, NAC International, Atlanta, GA.
- [4] LS-DYNA Keyword User's Manual – Volume I, Version 971, R8.0, LSTC, Livermore, California
- [5] ANSYS Mechanical User's Manual, Version 16, ANSYS INC, Canonsburg, PA
- [6] 2010 ASME Boiler and Pressure Vessel Code, Section III, Division 1, "Rules for Construction of Nuclear Facility Components", ASME, New York, NY.
- [7] 2010 ASME Boiler and Pressure Vessel Code, Section III, Division 3, "Containments for Transportation and Storage of Spent Nuclear Fuel and High Level Radioactive material and Waste", ASME, New York, NY
- [8] G. J. Bjorkman, "The New ASME Section III, Division 3 Strain-Based Acceptance Criteria and Computational Modeling Guidance Document" Technical Keynote, PATRAM 2013, San Francisco CA.
- [9] Snow, S. D., Morton, M.K, Pleins, E.L., Keating R., "Strain-Based Acceptance Criteria for Energy Limited Events", INL/CON-09-15609, Idaho National Laboratory, Idaho Fall, ID
- [10] 2010 ASME Boiler and Pressure Vessel Code, Section VIII, Division 2, "Alternative Rules, Rules for Construction of Pressure Vessels", ASME, New York, NY